

Modal content in hypocycloid Kagomé hollow core photonic crystal fibers

THOMAS D. BRADLEY,* NATALIE V. WHEELER, GREGORY T. JASION, DAVID GRAY, JOHN HAYES, MARCELO ALONSO GOUVEIA, SEYED R. SANDOGHCHI, YONG CHEN, FRANCESCO POLETTI, DAVID RICHARDSON, AND MARCO PETROVICH

Optoelectronics Research Centre, University of Southampton, Southampton, SO17 1BJ, UK

*tb1f13@soton.ac.uk

Abstract: The modal content of 7 and 19 cell Kagomé anti resonant hollow core fibers (K-ARF) with hypocycloid core surrounds is experimentally investigated through the spectral and spatial (S^2) imaging technique. It is observed that the 7 and 19 cell K-ARF reported here, support 4 and 7 LP mode groups respectively, however the observation that K-ARF support few mode groups is likely to be ubiquitous to 7 and 19 cell K-ARFs. The transmission loss of the higher order modes (HOMs) was measured via S^2 and a cutback method. In the 7 cell K-ARF it is found that the LP_{11} and LP_{21} modes have approximately 3.6 and 5.7 times the loss of the fundamental mode (FM), respectively. In the 19 cell it is found that the LP_{11} mode has approximately 2.57 times the loss of the FM, while the LP_{02} mode has approximately 2.62 times the loss of the FM. Additionally, bend loss in these fibers is studied for the first time using S^2 to reveal the effect of bend on modal content. Our measurements demonstrate that K-ARFs support a few mode groups and indicate that the differential loss of the HOMs is not substantially higher than that of the FM, and that bending the fiber does not induce significant inter modal coupling. A study of three different input beam coupling configurations demonstrates increased HOM excitation at output and a non-Gaussian profile of the output beam if poor mode field matching is achieved.

Published by The Optical Society under the terms of the [Creative Commons Attribution 4.0 License](https://creativecommons.org/licenses/by/4.0/). Further distribution of this work must maintain attribution to the author(s) and the published article's title, journal citation, and DOI.

OCIS codes: (060.4005) Microstructured fibers; (060.2300) Fiber measurements; (060.2270) Fiber characterization.

References and links

1. F. Poletti, N. V. Wheeler, M. N. Petrovich, N. Baddela, E. N. Fokoua, J. R. Hayes, D. R. Gray, and D. J. Richardson, "Towards high-capacity fibre-optic communications at the speed of light in vacuum," *Nat. Photonics* **7**(4), 279–284 (2013).
2. M. Triches, M. Michieletto, J. Hald, J. K. Lyngsø, J. Lægsgaard, and O. Bang, "Optical frequency standard using acetylene-filled hollow-core photonic crystal fibers," *Opt. Express* **23**(9), 11227–11241 (2015).
3. C. Wang, N. V. Wheeler, C. Fourcade-Dutin, M. Grogan, T. D. Bradley, B. R. Washburn, F. Benabid, and K. L. Corwin, "Acetylene frequency references in gas-filled hollow optical fiber and photonic microcells," *Appl. Opt.* **52**(22), 5430–5439 (2013).
4. Y. Y. Wang, X. Peng, M. Alharbi, C. F. Dutin, T. D. Bradley, F. Gérôme, M. Mielke, T. Booth, and F. Benabid, "Design and fabrication of hollow-core photonic crystal fibers for high-power ultrashort pulse transportation and pulse compression," *Opt. Lett.* **37**(15), 3111–3113 (2012).
5. B. Debord, M. Alharbi, L. Vincetti, A. Husakou, C. Fourcade-Dutin, C. Hoenninger, E. Mottay, F. Gérôme, and F. Benabid, "Multi-meter fiber-delivery and pulse self-compression of milli-Joule femtosecond laser and fiber-aided laser-micromachining," *Opt. Express* **22**(9), 10735–10746 (2014).
6. A. Urich, R. R. J. Maier, B. J. Mangan, S. Renshaw, J. C. Knight, D. P. Hand, and J. D. Shephard, "Delivery of high energy Er:YAG pulsed laser light at 2.94 μm through a silica hollow core photonic crystal fibre," *Opt. Express* **20**(6), 6677–6684 (2012).
7. Y. Chen, Z. Liu, S. R. Sandoghchi, G. T. Jasion, T. D. Bradley, E. N. Fokoua, J. R. Hayes, N. V. Wheeler, D. R. Gray, B. J. Mangan, R. Slavík, S. Member, F. Poletti, M. N. Petrovich, S. Member, and D. J. Richardson, "Multi - kilometer long, longitudinally uniform hollow core photonic bandgap fibers for broadband low latency data transmission," *J. Lightwave Technol.* **34**(4), 104–113 (2016).

8. G. T. Jasion, J. S. Shrimpton, Y. Chen, T. Bradley, D. J. Richardson, and F. Poletti, "MicroStructure Element Method (MSEM): viscous flow model for the virtual draw of microstructured optical fibers," *Opt. Express* **23**(1), 312–329 (2015).
9. F. Poletti, "Nested antiresonant nodeless hollow core fiber," *Opt. Express* **22**(20), 23807–23828 (2014).
10. W. Belardi and J. C. Knight, "Hollow antiresonant fibers with reduced attenuation," *Opt. Lett.* **39**(7), 1853–1856 (2014).
11. F. Benabid, J. C. Knight, G. Antonopoulos, and P. S. J. Russell, "Stimulated Raman scattering in hydrogen-filled hollow-core photonic crystal fiber," *Science* **298**(5592), 399–402 (2002).
12. J. R. Hayes, F. Poletti, M. S. Abokhamis, N. V. Wheeler, N. K. Baddela, and D. J. Richardson, "Anti-resonant hexagram hollow core fibers," *Opt. Express* **23**(2), 1289–1299 (2015).
13. F. Couny, F. Benabid, and P. S. Light, "Large-pitch kagome-structured hollow-core photonic crystal fiber," *Opt. Lett.* **31**(24), 3574–3576 (2006).
14. M. N. Petrovich, F. Poletti, A. van Brakel, and D. J. Richardson, "Robustly single mode hollow core photonic bandgap fiber," *Opt. Express* **16**(6), 4337–4346 (2008).
15. J. Jung, V. Sleiffer, N. Baddela, M. Petrovich, J. R. Hayes, N. Wheeler, D. Gray, E. R. Numkam Fokoua, J. Wooler, N. Wong, F. Parmigiani, S.-U. Alam, J. Suof, M. Kuschnerov, V. Veljanovski, H. Waardt, de, F. Poletti, and D. J. Richardson, "First demonstration of a broadband 37-cell hollow core photonic bandgap fiber and its application to high capacity mode division multiplexing," in *Optical Fiber Communication Conference/National Fiber Optic Engineers Conference 2013*, (2013), pp. 1–3.
16. D. R. Gray, M. N. Petrovich, S. R. Sandoghchi, N. V. Wheeler, K. Naveen, G. T. Jasion, T. Bradley, D. J. Richardson, and F. Poletti, "Real - time modal analysis via wavelength - swept spatial and spectral (S 2) Imaging," *IEEE Photonics Technol. Lett.* **28**(9), 1034–1037 (2015).
17. Y. Y. Wang, N. V. Wheeler, F. Couny, P. J. Roberts, and F. Benabid, "Low loss broadband transmission in hypocycloid-core Kagome hollow-core photonic crystal fiber," *Opt. Lett.* **36**(5), 669–671 (2011).
18. B. Debord, A. Amsanpally, M. Alharbi, L. Vincetti, J.-M. Blondy, F. Gerome, and F. Benabid, "Ultra-large core size hypocycloid-shape inhibited coupling Kagome fibers for high-energy laser beam handling," *J. Lightwave Technol.* **33**(17), 3630–3634 (2015).
19. B. Debord, M. Alharbi, T. Bradley, C. Fourcade-Dutin, Y. Y. Wang, L. Vincetti, F. Gérôme, and F. Benabid, "Hypocycloid-shaped hollow-core photonic crystal fiber part I: cladding Arc curvature effect on confinement loss," *Opt. Express* **21**(23), 28609–28616 (2013).
20. M. Alharbi, T. Bradley, B. Debord, C. Fourcade-Dutin, D. Ghosh, L. Vincetti, F. Gérôme, and F. Benabid, "Hypocycloid-shaped hollow-core photonic crystal fiber part II: cladding effect on confinement and bend loss," *Opt. Express* **21**(23), 28609–28616 (2013).
21. J. W. Nicholson, A. D. Yablon, S. Ramachandran, and S. Ghalmi, "Spatially and spectrally resolved imaging of modal content in large-mode-area fibers," *Opt. Express* **16**(10), 7233–7243 (2008).
22. J. W. Nicholson, A. D. Yablon, J. M. Fini, and M. D. Mermelstein, "Measuring the modal content of large-mode-area fibers," *IEEE J. Sel. Top. Quantum Electron.* **15**(1), 61–70 (2009).
23. D. R. Gray, S. R. Sandoghchi, N. V. Wheeler, N. K. Baddela, G. T. Jasion, M. N. Petrovich, F. Poletti, and D. J. Richardson, "Accurate calibration of S2 and interferometry based multimode fiber characterization techniques," *Opt. Express* **23**(8), 10540–10552 (2015).
24. B. Beaudou, A. Bhardwaj, T. D. Bradley, M. Alharbi, B. Debord, F. Gerome, and F. Benabid, "Macro bending losses in single-cell kagome-lattice hollow-core photonic crystal fibers," *J. Lightwave Technol.* **32**(7), 1370–1373 (2014).
25. T. D. Bradley, Y. Wang, M. Alharbi, B. Debord, C. Fourcade-dutin, B. Beaudou, F. Gerome, and F. Benabid, "Optical Properties of low loss (70dB / km) hypocycloid-core Kagome hollow core photonic crystal fiber for Rb and Cs based optical applications," *J. Lightwave Technol.* **31**(16), 2752–2755 (2013).
26. B. M. Trabold, D. Novoa, A. Abdolvand, and P. S. J. Russell, "Selective excitation of higher order modes in hollow-core PCF via prism-coupling," *Opt. Lett.* **39**(13), 3736–3739 (2014).
27. Y. Cheng, Y. Y. Wang, J. L. Auguste, F. Gerôme, G. Humbert, J. M. Blondy, and F. Benabid, "Fabrication and characterization of ultra-large core size (>100 μm) Kagome fiber for laser power handling," in *CLEO:2011 - Laser Applications to Photonic Applications* (2011), pp. 15–16.
28. N. K. Baddela, M. N. Petrovich, Y. Jung, J. R. Hayes, N. V. Wheeler, D. R. Gray, N. Wong, F. Parmigiani, E. Numkam, J. P. Wooler, F. Poletti, and D. J. Richardson, "First Demonstration of a low loss 37-cell hollow core photonic bandgap fiber and its use for data transmission," in *CLEO:2013 - Laser Applications to Photonic Applications* (2013).
29. T. G. Euser, G. Whyte, M. Scharrer, J. S. Chen, A. Abdolvand, J. Nold, C. F. Kaminski, and P. S. Russell, "Dynamic control of higher-order modes in hollow-core photonic crystal fibers," *Opt. Express* **16**(22), 17972–17981 (2008).

1. Introduction

Hollow core photonic crystal fibers (HC-PCFs) have become the subject of increasing interest as of recent, fueled by the progressive maturation of their fabrication technologies which bring the prospects of practical applications in telecommunications [1], laser frequency standards [2, 3] and, pulse delivery and compression [4–6] more sharply into focus. The wide

range of applications that can potentially be addressed by HC-PCFs has been facilitated by the development of two different families of HC-PCF with different structural and optical properties: Hollow Core Photonic Bandgap Fibers (HC-PBGF) [7, 8] and hollow core anti-resonant fibers (HC-ARFs) [9, 10]. Kagomé anti-resonant fibers (K-ARF) are a type of HC-ARF first reported in 2002 [11], which was significantly improved in 2011 through the addition of a hypocycloid core boundary [4], which resulted in a dramatic reduction in the attenuation. This development has since created new interest in novel HC-ARFs, particularly focused on achieving a negative curvature core boundary using simpler cladding structures in order to minimize resonances of the cladding, thus reducing the fiber loss [9, 12] and increasing the operable bandwidth. These recent developments, combined with other desirable properties of HC-ARFs such as low group velocity dispersion and large values of mode field diameter (MFD), have led to an increased uptake of these fibers in remarkable lab based demonstrations of high power pulse delivery and compression, gas sensing, metrology and nonlinear frequency conversion [13]. Despite the fact that it is well known that these fibers generally support multiple modes, and on the other hand most of the above mentioned applications critically rely on the beam quality, it is surprising that to date no detailed analysis of the modal properties of these fibers exists in the literature. As a comparison, the modal properties of HC-PBGFs are well understood with several detailed studies in this area [1, 14, 15].

Here, we present a first investigation of the modal content in K-ARF with 7 and 19 cell cores with a hypocycloid (negative curvature) core boundary. We investigate the transmission characteristics (attenuation and bend loss) of these fibers and, more importantly, we carry out an in-depth study of their modal content using a wavelength swept spatial and spectral (S^2) imaging technique [16]. This study confirms that both fibers are few-moded. Further, we report the first measurements of higher-order mode (HOM) attenuation in 7 and 19 cell K-ARF obtained via a cutback method in association with S^2 measurements. The results of this analysis show that non-zero HOM content is typically transmitted through tens of meters of fiber even under optimized launch conditions. Previous publications [5] have demonstrated that K-ARFs can be operated in an effectively single mode regime over meter lengths, but no detailed analysis of the full modal content was presented to confirm this. Additionally, bend loss in these fibers is studied for the first time using S^2 and the effect of bend on modal content is revealed. The impact of coupling conditions on the HOM content is also investigated, which clearly show the need for careful mode field matching to reduce HOM content and optimize coupling of light to the fundamental mode of the fiber.

2. Transmission and bend loss of Kagome anti-resonant fibers

Since the advent of hypocycloid K-ARF [17], there has been an interest in using these fibers for high power pulse delivery [4, 5, 18] because of their low loss, broad optical bandwidth, low group velocity dispersion, and the ability to operate the fibers in an effectively single mode regime [5]. The extremely large core sizes and thus MFD values achievable in K-ARF make them attractive for laser power delivery because of the very low overlap between the core-guided light and the silica surround, which is expected to lead to a substantial increase in laser induced damage threshold (LIDT). The increased arc curvature in 7 cell relative to 19 cell fiber designs allows lower loss to be achieved, however the larger core in a 19 cell design reduces the group velocity dispersion and for applications where gas filling/evacuation is necessary, the larger core dimension may speed up the filling time.

Figure 1 shows transmission, cutback loss and bend loss results obtained with a broadband white light source and an optical spectrum analyzer (OSA). Launching to the fundamental mode was optimized for the 7 and 19 cell K-ARFs through butt coupling to solid fibers with closely matched mode field diameters. The 7 cell K-ARF (Fig. 1(a)) used here supports broadband transmission in the first guidance band, spanning from 1350 – 1750 nm with a minimum loss of ~56 dB/km at 1541 nm. The 7 cell structure (inset Fig. 1(a)) has an inner

core diameter of $\sim 65 \mu\text{m}$ with $b = 0.59$ (curvature parameter defined in [19]) and a strut thickness of $\sim 600 \text{ nm}$ (measured from high resolution Scanning Electron Micrographs (SEMs)). The 19 cell K-ARF Fig. 1(b) has an inner core diameter (inset Fig. 1(b)) of $\sim 86 \mu\text{m}$ with $b = 0.49$ and a strut thickness $\sim 400 \text{ nm}$. This fiber guides in the first transmission band spanning 800 nm to 1750 nm , with an average loss of $\sim 160 \text{ dB/km}$ at 1550 nm and a minimum loss of $\sim 80 \text{ dB/km}$ at 980 nm (Fig. 1(b)). The 19 cell K-ARF reported here represents a state of the art (SOTA) fiber in terms of attenuation while the 7 cell K-ARF is comparable with the previously reported K-ARFs [4, 17]. Both 7 and 19 cell K-ARF demonstrate a broad transmission bandwidth, as commonly associated with K-ARFs, and a relatively flat transmission spectrum; our 7 cell fiber has a 3dB bandwidth exceeding 300 nm .

In addition to the transmission loss, we measured the bend loss of the 7 and 19 cell K-ARF; the spectral loss vs bend diameter of the two fibers are shown in Figs. 1(c) and 1(d). From Fig. 1(c) we see that the 7 cell K-ARF is relatively insensitive to bending for diameters up to approximately 12 cm . For bends tighter than 12 cm diameter the bend loss appears to increase rapidly at all wavelengths. In our 19 cell K-ARF a more pronounced wavelength dependence is also observed. At a bend diameter of 8 cm the bend loss at 1550 nm is $\sim 1.7 \text{ dB/m}$ but at 980 nm (close to the edge of the anti-resonant wavelength region) the bend loss increases to $\sim 7 \text{ dB/m}$. The 7 and 19 cell K-ARFs presented here both present good bending performance for diameters $> 12 \text{ cm}$ across the guidance band. Comparison with fibers reported in [18, 20] indicate that our fibers have similar transmission and bending performance.

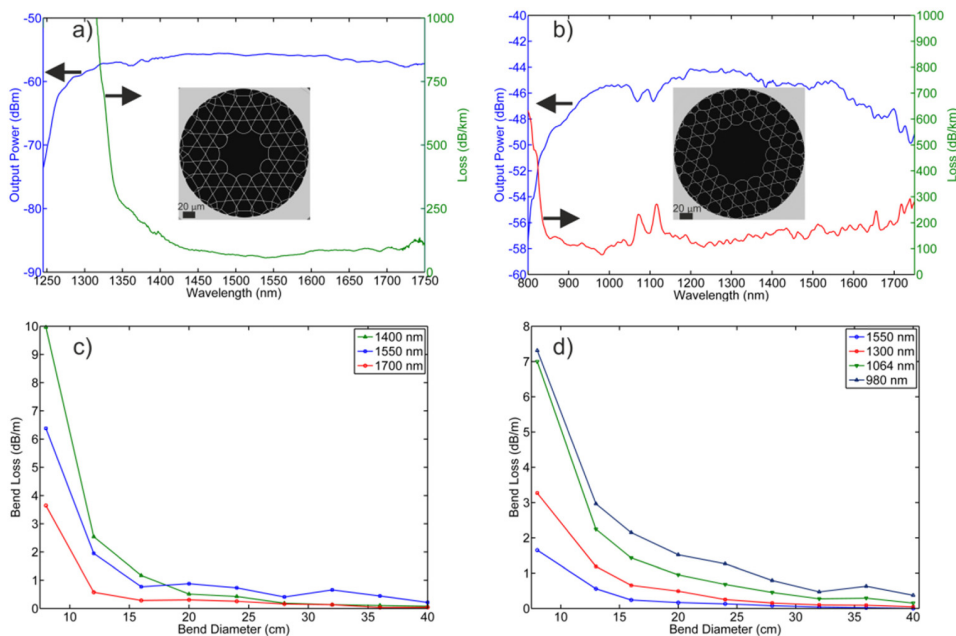


Fig. 1. 5 m Transmission (blue) and measured cutback loss curves (green) of a) 7 cell K-ARF and b) 19 cell K-ARF. Insets are SEMs of the transverse fiber structure. Bend loss for c) the 7 cell K-ARF and d) the 19 cell K-ARF. OSA resolution = 10 nm for all measurements.

3. Spatial and spectral imaging setup

The S^2 setup is shown in Fig. 2 [21, 22]. It incorporates a tunable laser source (TLS, range $1520 - 1630 \text{ nm}$) with a minimum step size of 1 pm which is delivered through a single mode fiber (SMF). A single aspheric lens is used to collimate the light from the SMF delivery fiber and a $5\times$ magnification microscope objective is used to couple light into the fiber under test

(FUT) with an approximate focused spot size of $\sim 58 \mu\text{m}$. A series of two half wave plates and a polarizing beam splitter provide for power/polarization control before the light is coupled into the FUT. An InGaAs CCD array, directly triggered by the TLS and controlled by a PC collects the output from the FUT through a telescope. Data acquisition and analysis are controlled from the PC [23]. The calibration techniques detailed in [23] have been implemented in this system to ensure the greatest possible measurement accuracy.



Fig. 2. Spatial and spectral (S^2) imaging setup. TLS: Tunable Laser Source, SMF: Single Mode Fiber, HWP: Half-wave plate, PBS: Polarizing beam splitter, CCD: InGaAs camera, Lenses shown by double headed arrows.

4. 7 cell Kagome anti-resonant fiber

The ability to operate 7 cell K-ARFs in an effectively single mode regime when input coupling is optimized has led various groups to implement these fibers in pulse delivery and compression experiments. However, to the best of our knowledge, no detailed modal characterization has been carried out on this type of fiber, nor has the differential mode loss ever been investigated experimentally in 7 and 19 cell hypocycloid core K-ARF.

4.1 Modal content in a loosely coiled fiber

Initial S^2 measurements were carried out on 31.5 m of 7 cell K-ARF loosely coiled with a diameter of ~ 30 cm on the optical bench. A free space launch was used (Fig. 2) and coupling to the fundamental mode was optimized through real-time analysis with our S^2 setup [16]. During the alignment, the polarization optics were optimized to control the power coupled to the fundamental mode and avoid saturation of the CCD array. In Fig. 3(a) the typical multipath interference (MPI) vs. differential group delay (DGD) curve from the S^2 measurement performed on a 31.5m length of K-ARF over a 20 nm bandwidth (1540 – 1560 nm, 1 pm resolution) is shown. Six peaks are readily observable in the DGD range $\sim 0.5 - 2$ ps/m and are marked with letters A-F in Fig. 3(a). The mode intensity and phase profiles associated with these peaks (A-F) are shown in Fig. 3(b). In addition to the fundamental mode, LP_{11} , LP_{21} , LP_{02} and LP_{31} mode groups can be seen. The feature at DGD values of ~ 2.5 ps/m is a measurement artifact due to double reflections of core guided modes from optical components within the setup [23]. The first LP_{11} mode has an MPI value of ~ -16.5 dB, while the remaining modes have MPI values ranging from -15.8 to -45 dB.

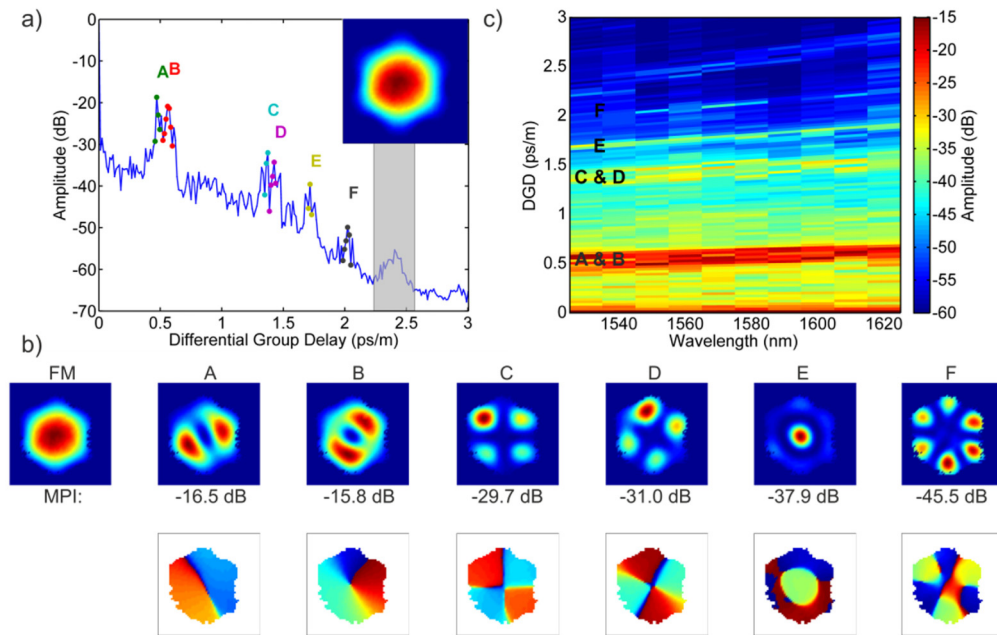


Fig. 3. S^2 analysis of the 7 cell K-ARF. a) Differential group delay and relative power of higher order modes (MPI), inset: beam profile summed across all wavelengths, b) Experimental S^2 mode intensity and phase profiles, and c) Spectrogram measurement across 110 nm wide range covered by our source (1520-1630 nm).

Two conclusions can be drawn immediately from this result: firstly, it is confirmed that 7 cell K-ARFs are not rigorously single mode; furthermore, the two LP_{11} higher order modes (HOMs) observed are guided through the full length of fiber used here contributing a significant fraction of the total output power (~ 2.2 to 2.6% of the total optical power). By collecting multiple S^2 measurements over adjacent regions of 10 nm width (10 pm resolution), a spectrogram covering the range 1520 – 1630 nm was obtained, which shows the wavelength dependence of the MPI and DGD, as shown in Fig. 3(c). Here, the various mode groups are visible as distinct linear regions of high intensity with approximately linear dependence on the wavelength (for all modes the DGD increases with increasing wavelength). In Fig. 3 the DGD range is curtailed at 3 ps/m because no further modes with higher DGD are guided and thus the signal level drops to the noise floor at -70 dB. Further, all the modes observed in Fig. 3(a) and 3(b) can be observed at all wavelengths within the spectrogram suggesting that this 7 cell K-ARF may support at least 4-5 mode groups across the full low loss transmission bandwidth of the first guidance band (Fig. 1(a)).

4.2 Modal content in a tightly coiled fiber

One of the primary advantages of an optical fiber is the ability to coil it to reduce the physical footprint for use in compact devices. In Section 1.1 the bend loss of the 7 cell K-ARF was reported to be approximately 6.5 dB/m, measured at 1550 nm with an 8 cm bend diameter. While previous work [24, 25] has documented the coupling to cladding modes under tight bending, to the best of our knowledge no study has been undertaken to determine the intermodal coupling of core guided modes under bending.

Here, three unique scenarios are considered firstly a tight 5cm diameter full coil is applied at the fiber input, secondly loosely coiled fiber and finally a tight 5cm diameter full coil is applied to the fiber output. Such a tight coil can induce mode coupling, however the turn at the input will allow any coupled light to propagate through the full length of the fiber.

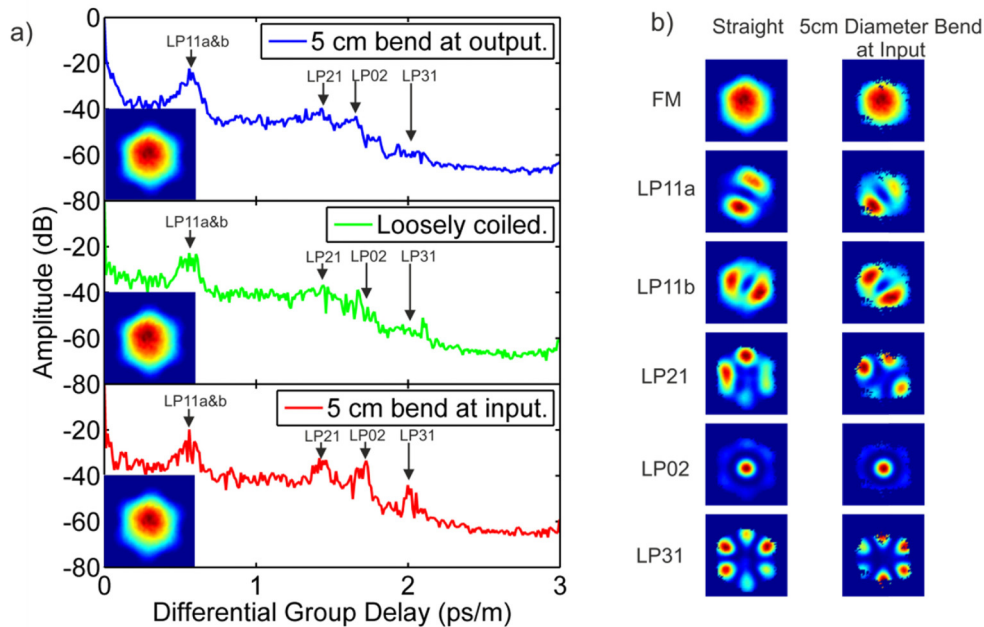


Fig. 4. a) DGD of 7 cell K-ARF with a 5 cm full coil at the output (blue) loosely coiled (green) and a 5 cm bend at the input (red). Inset: beam profile summed over all wavelengths for each bending configuration. b) S^2 mode profiles for a straight and a 5cm coil at the input.

In Fig. 4(a), the DGD is plotted for a 31.5 m length of K-ARF loosely coiled (central panel in Fig. 4(a)), and with a 5 cm diameter bend located close to the input (bottom panel), and the output of the fiber (top panel), respectively. In Fig. 4(a), it is apparent that the tight bending at the input and the output does not alter the measured DGD values of the HOMs, as expected; more interestingly, it does not induce coupling to any additional HOMs from those supported in the loosely coiled fiber. For a 5 cm diameter bend imposed at the fiber input, the peaks due to the LP₂₁ and LP₀₂ modes (at DGDs of ~ 1.4 ps/m and 1.7 ps/m respectively) increase in magnitude, which indicates power being transferred to these modes due to the perturbation caused by the tighter bend. The MPI increases from ~ 32 dB to -29 dB for LP₂₁ and from ~ 35 dB to -32 dB for LP₀₂, respectively. A 5 cm diameter bend at the output created no discernable increase in coupling to HOMs than the loosely coiled case. From comparison of the mode intensity profiles extracted from the S^2 measurement shown in Fig. 4(b), it is clear that for a loosely coiled fiber and a fiber under tight bending the guided modes are not significantly distorted. Tight coiling at the input of the 7 cell K-ARF induces coupling to the LP₂₁ and LP₀₂ modes, however there is no significant coupling between the other HOMs nor does it increase distributed coupling along the fiber length.

4.3 Higher order mode loss

In Section 4.1 and 4.2 the modal content in a 7 cell K-ARF has been investigated in both loosely coiled and under tight bending conditions; observation of the power distribution of the reconstructed modes via the S^2 imaging technique, and also consideration of the fact that they are observed after 31.5 m of fiber, leads us to conclude that in both scenarios the HOMs are strongly guided by the fiber and do not appear to leak significantly into the cladding. This observation suggests that the HOMs in K-ARF are unlikely to have significantly higher differential loss as compared to the fundamental mode. In order to demonstrate this experimentally, a differential S^2 measurement by fiber cutback was performed. An S^2 measurement with 20 nm bandwidth (1540 – 1560 nm) and a 1 pm resolution was carried out

for three different fiber lengths (31.5 m, 10 m and 5 m) whilst very accurately maintaining the same launch conditions into the fiber.

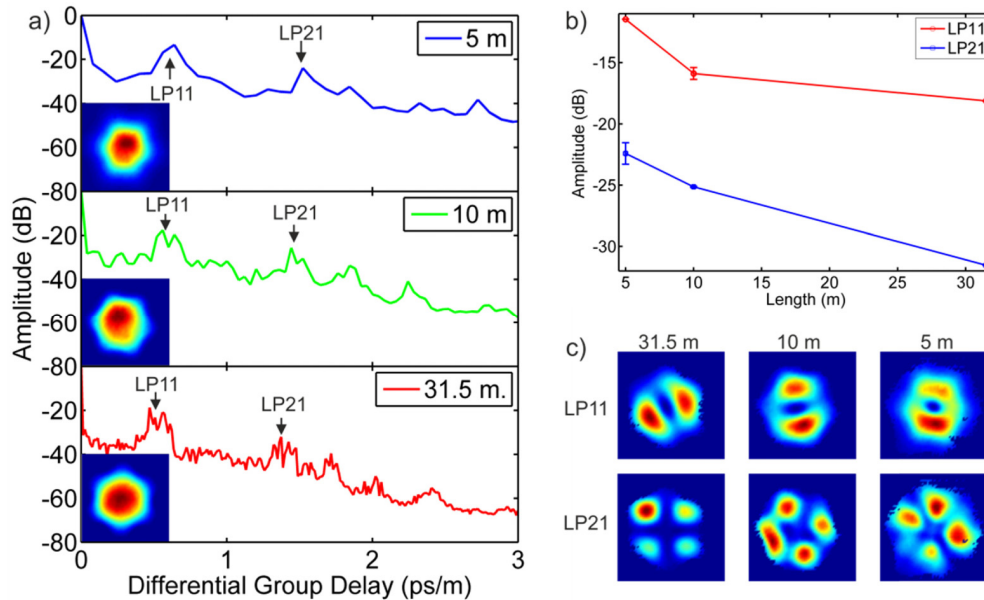


Fig. 5. a) Length-dependent DGD curves for 31.5 (red), 10 (green) and 5 m (blue) of 7 cell K-ARF (fixed launch conditions). Inset: beam profiles summed over all wavelengths for each cutback length. b) MPI of LP₁₁ and LP₂₁ HOMs as a function of fiber length. Error bars are the standard deviation of three S² measurements at each fiber length (repeat cleaves). c) S² mode profiles at the different cutback lengths. Note that the orientation of the modes in the images changes because after each cut the fiber is repositioned at a slightly different orientation on the output coupling v-groove

The DGD curves are shown in Fig. 5(a) for the 7 cell K-ARF as the sample length is cutback from 31.5 m to 10 m and to 5 m. As expected, from Fig. 5(a) it is apparent that the noise floor of the system increases and the DGD resolution decreases with decreasing length. Although not readily apparent from Fig. 5(a), the MPI values of the discrete HOMs also increase as the length is reduced, as shown for the LP₁₁ and LP₂₁ modes in Fig. 5(b), here the MPI has been corrected to account for the fiber loss. Calculating the gradient from Fig. 5(b) allows the loss of the LP₁₁ mode to be estimated as $\approx 208 \pm 60$ dB/km and the LP₂₁ mode loss can be estimated at $\approx 330 \pm 40$ dB/km. Comparison with the loss measured by cutback in Fig. 1, which demonstrates a minimum loss of ~ 56 dB/km at 1541 nm, shows that the loss values of the HOMs are 3.7 and 5.8 times higher than the fundamental mode. The series of measurements reported above show that 7 cell K-ARF are few moded, and that the HOMs are strongly confined to the core with relatively low loss. The mode profiles for the LP₁₁ and LP₂₁ mode at the different cutback lengths are shown in Fig. 5(c), and the modes are clearly identifiable.

4.4 Impact of launch conditions on HOM content

Lastly, we use the S² technique to investigate the impact of different coupling conditions on the HOM content propagating in the 7 cell K-ARF. This fiber has an estimated MFD ~ 51 μm . Three different coupling setups were investigated: the first was the free space lens launch used for the previous measurements, which had a focused spot size ~ 58 μm ; the second and third are butt coupling (BC) with a single mode fiber (SMF-28, MFD $\sim 10.4 \pm 0.1$ μm at 1550 ± 10 nm) and an endlessly single mode photonic crystal fiber (LMA-35 from NKT Photonics)

with MFD $\sim 26 \mu\text{m}$ which is invariant with wavelength. From the experimentally recorded mode profiles the MFD of the K-ARFs is nearly invariant across the measurement bandwidth. SMF-28 and LMA-35 are chosen as examples of commercially available fibers which are often used for BC launch into K-ARFs.

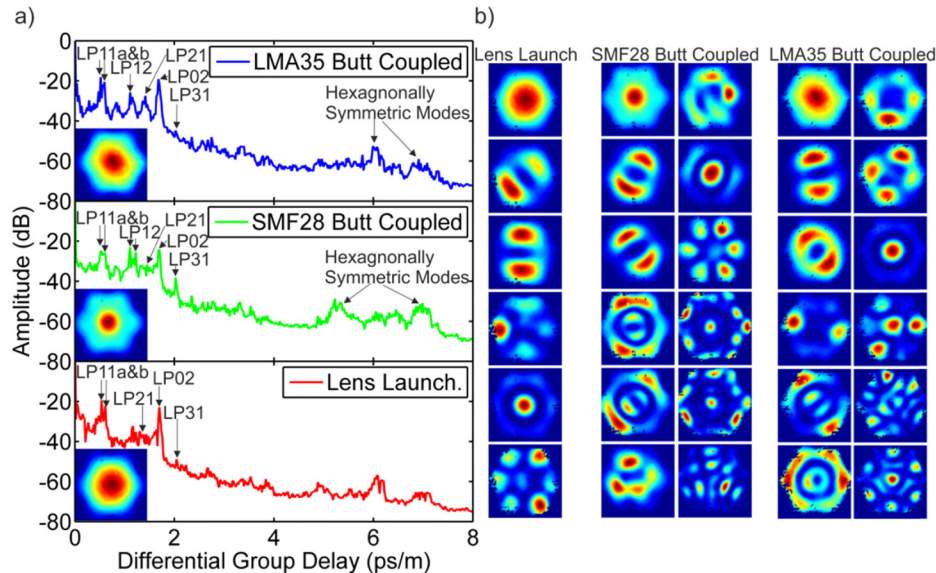


Fig. 6. a) DGD curves for free space lens launch (red), butt coupling with SMF-28 (green) and LMA-35 (blue) through 21 m of 7 cell K-ARF. Inset: beam profiles summed over all wavelengths for each launch condition. b) S^2 mode profiles for the three different coupling conditions.

We can see from the DGD plots (Fig. 6(a)) that the free space lens launch excites fewer HOMs than the SMF-28 and LMA-35 butt coupling. This is particularly apparent in the DGD range from 0.5 – 2 ps/m, where there are more peaks indicating discrete HOMs launched in the fiber. Study of the HOM profiles (Fig. 6(b)) when launching with SMF-28 and LMA-35 fiber reveals that the LP_{12} mode is more strongly excited compared to the case of a free space launch. Additionally, the butt coupling launch excite hexagonally symmetric modes which are not readily recognizable through the LP mode descriptions similar modes have been observed through side prism coupling techniques [26]. The fundamental mode profiles for the three different launch conditions are markedly different, with the free space lens launch providing the most symmetric and central excitation of the fundamental mode. The LMA-35 provides a reasonable excitation of the fundamental mode, albeit with some ellipticity due to imperfect mode matching at the launch. When launching with the SMF-28, the dominantly excited mode and beam profile are LP_{02} -like with an intense central lobe. Due to the increased HOM content excited by this launch condition, the S^2 algorithm is inaccurate and thus absolute MPI values for the HOMs cannot be measured but a significant increase in HOM content can be observed compared to the lens launch. This intense central lobe has a Gaussian profile and could be misinterpreted as the fundamental mode. When launching with an SMF-28 the dominantly excited mode is not LP_{01} . The likely reason for this is the large MFD mismatch of the fundamental mode between SMF-28 (MFD $\sim 10.4 \mu\text{m}$) and the K-ARF (MFD $\sim 51 \mu\text{m}$). From this series of measurements, we see that poor MFD matching at the launch increases the HOM content and decreases coupling to the fundamental mode of the 7 cell K-ARF. Increased HOM content induced from the launch conditions will have an impact both on fiber characterization and potentially on some of the applications proposed for K-ARFs.

5. 19 cell Kagome hollow core fiber

19 cell K-ARF have also recently found applications in laser power handling [18]. As compared to 7 cell K-ARFs, 19 cell K-ARF can achieve significantly larger core diameters, with greater than 100 μm demonstrated [27]. This increase in core size will reflect in a larger MFD but is also expected to impact the modal content. Again, however, no detailed experimental investigation has been made into the modal content of this type of fiber beyond the brief theoretical analysis presented in [18].

5.1 Modal content in a loosely coiled fiber

The modal content in the 19 cell K-ARF was investigated in a similar manner as described in section 4 for the 7 cell K-ARF. Figure 7(a) shows the result of a single measurement performed on a 30 m length of 19 cell K-ARF, loosely coiled, with 20 nm measurement bandwidth (1540 – 1560 nm) and 1 pm resolution.

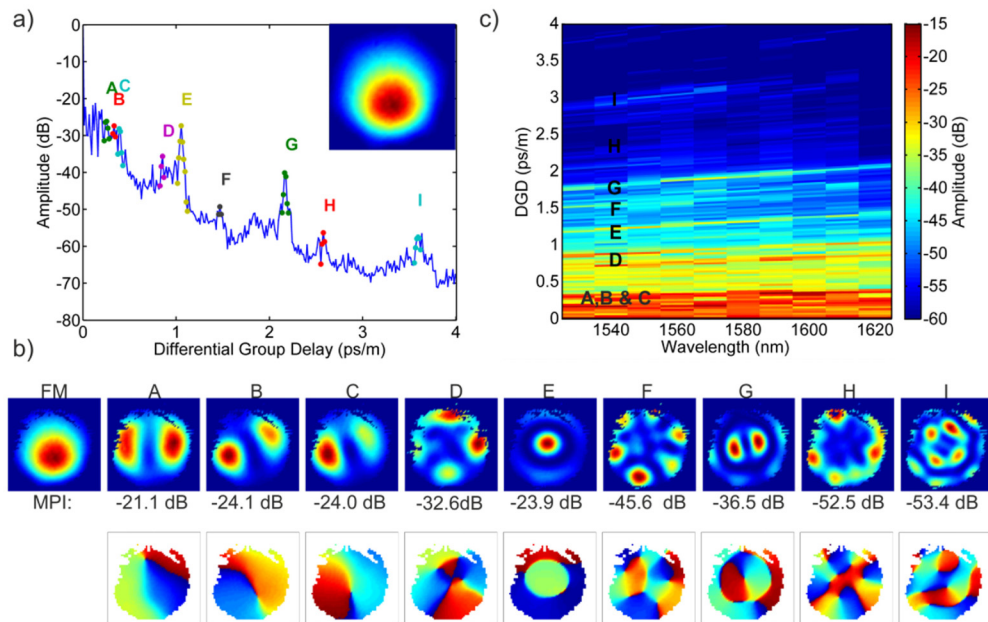


Fig. 7. S^2 results of the 19 cell K-ARF a) DGD curve for 30 m of 19 K-ARF, inset: beam profile summed across all wavelengths, b) S^2 mode intensity and phase profiles propagating in 19 cell K-ARF, c) Spectrogram of the HOM content in 19 cell K-ARF.

In addition to the fundamental mode, nine HOM groups, identified as LP_{11} , LP_{21} , LP_{02} , LP_{31} , LP_{12} , LP_{41} and LP_{42} , can be observed (peaks labelled A to I in Fig. 7(a) and 7(b)) - the relevant intensity and phase profiles can be observed in Fig. 7(b)). This demonstrates that the 19 cell supports as expected more HOMs as compared to the 7 cell fiber. Similarly to the 7 cell fiber, the modes are guided through the fiber over the 30 m, suggesting that they do not suffer significantly higher attenuation than the fundamental mode. The $LP_{11a,b}$ modes have MPI values of \sim -21 dB to -24 dB, with the weakest HOM group (I in Fig. 7(a)) having MPI value of \sim -54 dB. All the HOMs have low DGDs, lower than 5 ps/m. Such behavior correlates with an increased core diameter and has previously been observed in 37 cell HC-PBGF [28]. Figure 7(c) shows a spectrogram of the modal content in the 19 cell K-ARF; HOMs span the full spectrogram with the modes at short DGD exhibiting large MPI. Beyond the nine guided core mode groups observed at low DGDs the remaining spectrum is clear, i.e. no further mode is observed. Given the extremely large core of this fiber (86 μm) it is unsurprising that several HOM groups are supported, however it is clear that these modes are

well confined in the core and are guided through the whole length of the fiber and appear to extend across the entire transmission band as was the case in the 7 cell K-ARF. In [18], Debord et al. comment on the fact that large core design K-ARFs support HOMs and show numerical simulations of the loss evolution with the degree of negative curvature but no experimental data has been presented until now.

5.2 19 cell Kagome ARF: modal content in a tightly coiled fiber

In consideration of the fact that larger core sizes normally correlate with a stronger bend sensitivity (in both conventional and micro-structured fibers), it is important to investigate the impact of bending on the modal content in the 19 cell K-ARF.

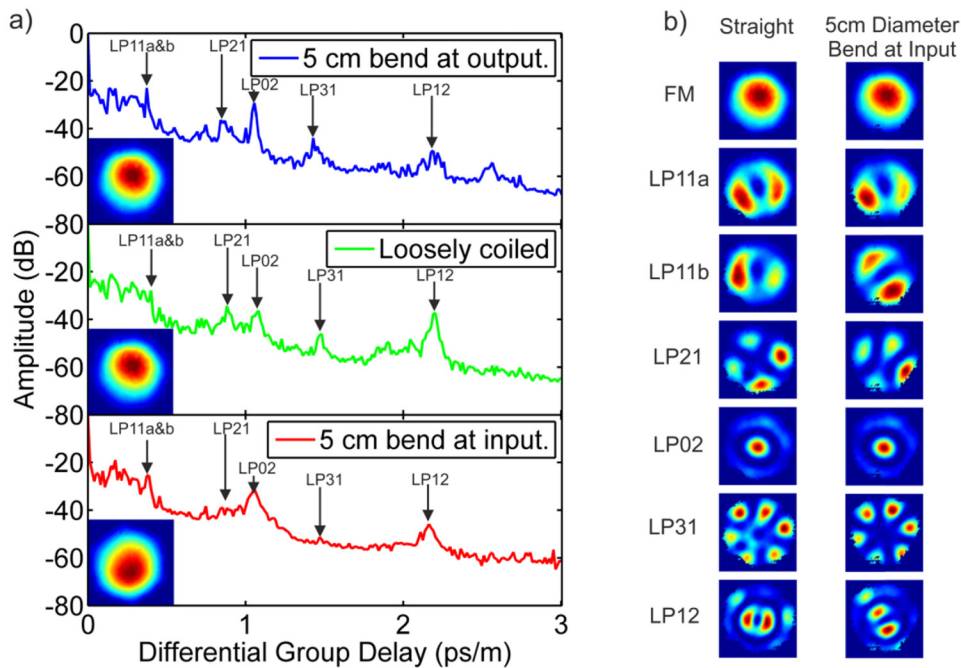


Fig. 8. a) DGD curves for 30 m of 19 cell K-ARF with 5 cm diameter bend at input (red), output (blue), and effectively straight (green). Inset: beam profile summed over all wavelengths for each bending configuration. b) S^2 mode profiles in a straight fiber and with 5 cm diameter bend at input.

Figure 8(a) shows the result of a similar set of measurements as presented in Section 4.2 for the 7 cell K-ARF. The DGD curves (Fig. 8(a)) are shown for a 30 m length of loosely coiled (30 cm diameter) 19 cell K-ARF (middle panel), and with a 5 cm diameter bend at the input and the output of the fiber (bottom and top panel, respectively). Figure 8(a) shows that the LP_{12} mode at a DGD ~ 2.1 ps/m demonstrates a reduction in MPI value from ~ 34 dB to ~ 46 dB from the loosely coiled to tightly bent configurations. The LP_{31} mode at DGD ~ 1.5 ps/m experiences a reduction of MPI from ~ 41 dB to ~ 47 dB when a tight 5 cm coil is applied at the input. Tight coiling at the output has minimal impact on the modal content. The associated mode intensity profiles for the straight and bent fiber are shown in Fig. 8(b); all the mode fields are recognizable but some are distorted. From Fig. 8(a) it is apparent that bending causes increased loss of some of the HOMs, for example LP_{12} and LP_{31} , but it doesn't cause excitation of HOMs which are not supported in the loosely coiled fiber. In [24, 25] bend loss is attributed to a coupling mechanism between core modes and those which are supported in the air holes of the cladding, which are lossy. Remarkably for such a large MFD fiber the impact of bending on inter-modal coupling is relatively minor. However, the impact of

bending is greater than in the 7 cell K-ARF with a larger change in the MPI for some modes. Given the larger core diameter of the 19 cell compared to the 7 cell (86 μm compared to 65 μm) it is unsurprising that bending has a greater impact on the modal content.

5.3 19 cell Kagome ARF: higher order mode loss

From Sections 5.1 and 5.2, it is obvious that the HOMs in this 19 cell K-ARF are well guided in the fiber and are relatively insensitive to bending, this is quite a striking result. This raises the question as to what is the loss of the HOMs in 19 cell K-ARF. A cutback measurement of the 19 cell K-ARF is carried out, in which S^2 measurements are collected for 30 m to 10 m to 5m long samples while maintaining the input coupling conditions as accurately as possible. Single shot measurements with a 20 nm bandwidth (1540 –1560 nm) and 1 pm resolution were obtained at each fiber length.

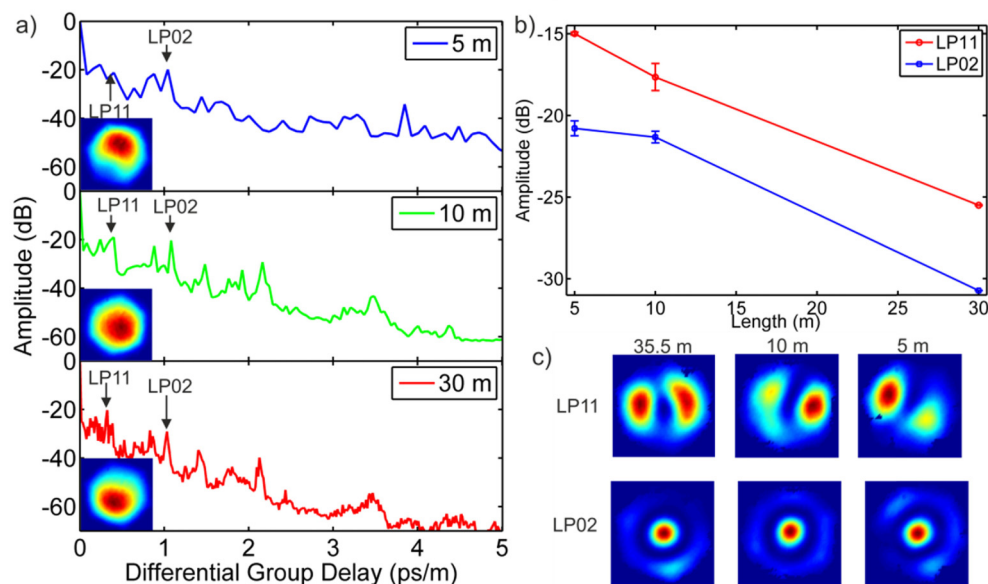


Fig. 9. a) DGD curves for 31.5 m (red), 10 m (green) and 5 m (blue) lengths of 19 cell K-ARF. Inset: beam profiles summed over all wavelengths for each cutback length. b) MPI corrected for fiber transmission loss for the LP₁₁ (red) and LP₀₂ (blue) modes at different cutback lengths. Error bars are the standard deviation of three measurements at each length. c) S^2 mode profiles at cutback positions.

In Fig. 9(b) the MPI values corrected for the fiber transmission loss of the LP₁₁ and LP₀₂ modes are plotted for the different fiber lengths, providing a loss estimate of $\sim 412 \pm 23$ dB/km for the LP₁₁ and $\sim 418 \pm 60$ dB/km for the LP₀₂ modes. The standard cutback measurement in Fig. 1(b), which predominantly measures the loss of the fundamental mode, estimates the fundamental mode loss to be ~ 160 dB/km at 1550 nm. These measurements suggest that the LP₁₁ mode has 2.57 times the loss of the fundamental mode while the LP₀₂ mode is ~ 2.62 times higher. In Fig. 9(c), the mode profiles for the LP₁₁ and LP₀₂ modes are shown, illustrating that, while there is some perturbation of the mode fields at different lengths the modes are still readily recognizable at all lengths. While the HOMs contain $\sim 1\%$ of the total guided power through the fiber length of ~ 30 m the loss of these HOMs is only 2.6 times higher than that of the fundamental mode. Note that for short fiber lengths the DGD resolution is low thus only the dominant modes can be measured.

5.4 19 cell Kagome ARF: Impact of launch conditions on HOM content

Similar to Section 4.4, different coupling conditions are investigated. In this case the 19 cell K-ARF has an estimated MFD $\sim 67 \mu\text{m}$. A telescope based free space launch with a input spot size $\sim 58 \mu\text{m}$, is used and compared as before to butt coupling to SMF-28 BC and an LMA-35. Comparison of the DGD plots (Fig. 10) for the different launch conditions demonstrate that again significantly more modal content is excited through BC with an SMF-28 and an LMA-35 relative to the free space launch. The free space launch results in less HOMs, but as compared to the 7 cell K-ARF, more overall HOM content is excited. For the SMF-28 and LMA-35 BC multiple peaks are observed in the DGD range $0.5 - 2.5 \text{ ps/m}$, which are not observed when free space launching. These peaks have an MPI comparable to the HOMs excited in the free space launch.

In Fig. 10(b) the HOMs are presented for the three different coupling conditions. For the SMF-28 and the LMA-35 the lower order LP modes are distorted compared to the free space launch. Additional modes with more complex spatial distributions are excited through the BC.

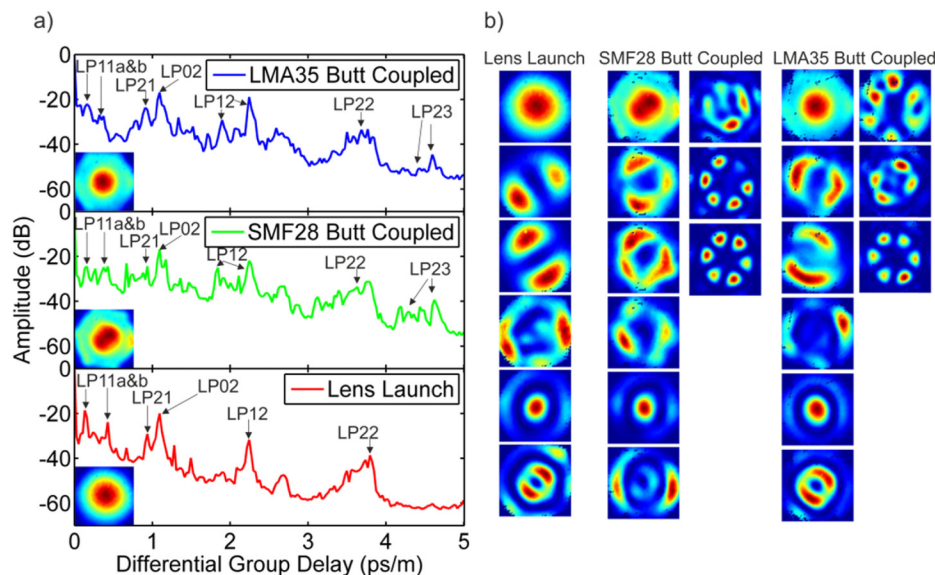


Fig. 10. a) DGD curves for free space lens launch (red), butt coupling to SMF-28 (green) and LMA-35 (blue) through 25.5 m of 19 cell K-ARF. Inset: beam profiles summed over all wavelengths for each launch condition. b) S^2 mode profiles for the three different coupling conditions.

Through free space launch the dominant mode is unequivocally the LP01 with an estimated MFD of $\sim 67 \mu\text{m}$. In the case of the SMF, the S^2 reconstructed mode profile yields a non-Gaussian intensity profile with an intense central lobe. We speculate that this is due to the fact that LP01 is not the dominant mode excited and thus the basic assumption for the S^2 does not hold anymore. Given the application of 19 cell K-ARF for laser power delivery and gas sensing, it is clear from the above results that careful selection of launch conditions are necessary to avoid the detrimental effects of modal interference and mode perturbation.

6. Discussion of modal content in K-ARF

A detailed modal characterization of 7 and 19 cell K-ARF with hypocycloid core boundary has been presented. A summary of the findings for the HOM loss of the two fibers is given in Table 1. We can see that the HOMs have increased attenuation compared to the fundamental mode but only of the order of 2 – 5.7 times higher. This means that, whilst, as experimentally observed, these fibers can be operated in an effectively single mode regime through careful

input launch, any HOMs excited at launch can in principle be transmitted over length scales if a few tens of meters as differential loss is not high enough to completely suppress them, and even for the best mode matched launch we could realize, HOM content of about 1 - 3% was observed. Such content will have an impact for some applications such as sensing, and may even have a detrimental impact upon the pointing stability of laser beam delivery system in some instances.

From the S^2 measurements taken separately for 5 cm diameter turns at the input and output of the 7 and 19 cell K-ARF, it is apparent that such bends do not induce significant mode coupling despite the fact that the core diameter of these fibers is large (65 μm & 86 μm). This is a significant result for fibers which have application in laser pulse delivery and compression, where the flexible nature of a fiber is beneficial.

Table 1. Mode dependent loss in 7 and 19 cell core K-ARF.

	7 cell	19 cell
Core Diameter (μm)	65	86
LP ₀₁ (dB/m)	0.056 \pm 0.01	0.16 \pm 0.01
LP ₁₁ (dB/m)	0.208 \pm 0.06	0.41 \pm 0.02
LP ₂₁ (dB/m)	0.33 \pm 0.04	-
LP ₀₂ (dB/m)	-	0.42 \pm 0.06

The mode dependent loss has been investigated previously in single cell K-ARF which have smaller cores and typically no negative curvature; in such fibers the fundamental and the HOM loss has been reported as being significantly larger than the values found here [26, 29].

Finally, the impact of different launching conditions in both the 7 and 19 cell K-ARF has demonstrated that poor mode field matching results in significantly increased HOM content being launched in both fiber types. More significantly poor MFD matching results in a non-Gaussian mode being excited as the dominant mode, this combined with the increased HOM content poses serious complications for even the simplest measurement such as the optical cutback technique. These observations are indicative that beam coupling to 7 and 19 cell K-ARF should aim to achieve the best possible mode match.

7. Conclusion

A 7 cell K-ARF with a 65 μm diameter core, negative curvature parameter $b = 0.59$, a strut thickness of ~ 600 nm and a loss of ~ 58 dB/km at 1541 nm has been reported. Secondly, a 19 cell K-ARF with an 86 μm diameter core, $b = 0.49$, a strut thickness ~ 400 nm and a loss of ~ 160 dB/km at 1550 nm has been fabricated. Both fibers demonstrate close to SOTA performance in terms of both transmission and bend loss compared to previously reported K-ARF. Here, the modal content of the 7 and 19 cell K-ARF has been investigated by means of the S^2 imaging technique. It has been conclusively shown for the first time that both 7 and 19 cell K-ARF support propagation of a few mode groups through lengths of a few tens of meters and that these HOM are relatively insensitive to bending for bend diameters > 12 cm. Bending does not induce significant intermodal coupling despite the large core diameters in these 7 and 19 cell K-ARFs. In the 7 cell K-ARF the traditional cutback measurement yields a loss value ~ 56 dB/km at 1550 nm and an S^2 cutback estimates the loss of the LP₁₁ and LP₂₁ modes at 208 dB/km and 330 dB/km respectively. Here, we see for the first time that not only are 7 cell K-ARF few-moded but also that the HOMs do not suffer significantly higher propagation losses as compared to the fundamental mode. In the 19 cell similar behavior is observed with a standard cutback loss estimate of ~ 160 dB/km (at 1550nm) and S^2 cutback estimating the LP₁₁ and LP₀₂ losses at 412 dB/km and 418 dB/km respectively. The striking result here is that the losses for these HOMs are a maximum 5.8 times higher than the fundamental mode loss. This improved understanding of the modal content in K-ARF will inform future investigations in pulse delivery and compression, and frequency stabilization in this class of fibers. Finally it has been shown that non-optimized launch conditions have a detrimental impact on the HOM content and the spatial distribution of the output beam profile

in 7 and 19 cell K-ARF. Thus in order to ensure accuracy in all measurements care should be taken to achieve an optimal launch which minimizes the MFD mismatch into 7 and 19 cell K-ARF. From the results presented here, it is apparent that 7 and 19 cell K-ARF are not rigorously single mode but the level of HOM content maybe tolerable for some applications such as power delivery where the fibers can be operated in an effectively single mode regime. However, for frequency standards, gas sensing and interferometric applications such as gyroscopes the level of HOM content observed here is likely to be detrimental to these applications. Given the recent uptake of this class of fibers it is necessary to understand the full modal characteristics to ensure optimal performance in the targeted application.

Acknowledgments

This work was supported), by the UK EPSRC through grant numbers EP/H02607X/1 (EPSRC Centre for Innovative Manufacturing in Photonics). The data for the plots in this paper can be found at <http://dx.doi.org/10.5258/SOTON/389700>.